

# Approaching the ground state of the kagomé antiferromagnet

W. Schweika,<sup>1</sup> M. Valdor,<sup>2</sup> and P. Lemmens<sup>2</sup>

<sup>1</sup> Institut für Festkörperforschung, Forschungszentrum Jülich, D-52425 Jülich, Germany

<sup>2</sup> Institut für Physik der Kondensierten Materie, TU Braunschweig, D-38106 Braunschweig, Germany  
(Dated: January 7, 2019)

$Y_{0.5}Ca_{0.5}BaCo_4O_7$  contains kagomé layers of  $Co^{3+}$  ions, whose spins are strongly coupled according to a Curie-Weiss temperature of  $\sim 2200$  K. At low temperatures,  $T = 1.2$  K, our diffuse neutron scattering study with polarization analysis reveals characteristic spin correlations close to a predicted two-dimensional coplanar ground state with staggered chirality. The absence of three-dimensional long-range AF order proves negligible coupling between the kagomé layers. The scattering intensities are consistent with high spin  $S = 3/2$  states of  $Co^{3+}$  in the kagomé layers and low spin  $S = 0$  states for  $Co^{3+}$  ions at interlayer sites. Our observations agree with previous Monte Carlo simulations indicating a ground state of only short range chiral order.

PACS numbers: 75.25.+z, 75.40.Cx, 75.50.Ee

In low dimensions, antiferromagnetic (AF) order is suppressed at finite temperatures [1] and geometrical frustration raises the complexity of ground states with finite entropy and non-collinear, chiral spin structures [2]. Spin chirality is related to unique universality classes [3, 4] and has relevance for the spin excitations in copper-oxide superconductors [5, 6]. A challenge for theoretical understanding for decades is the utmost frustration among AF coupled spins on the two-dimensional kagomé lattice [7].

Considering the configurational energy of the classical Heisenberg AF,

$$H = \sum_{\langle i,j \rangle} J(\mathbf{r}) \mathbf{S}_i \cdot \mathbf{S}_j; \quad (1)$$

for AF interaction to only nearest neighbors,  $J(\mathbf{r}_{ij}) > 0$ , the ground state is highly degenerate. There are two competing ordered coplanar spin structures (see Fig. 1), with relative spin orientations of 120 degrees, which are either of uniform or staggered chirality. We use the convention that the chirality is positive when the spins rotate in steps of 120 degrees as one goes around a triangle. Apart from the degeneracy of a common in-plane spin rotation, there are further degeneracies related to possible local disorder, as shown in Fig. 1. Within its configurational space, thermal fluctuations [10, 11] as well as quantum fluctuations [8] select the  $\sqrt{3} \times \sqrt{3}$  structure. The entropically selection resolving a ground state degeneracy is a mechanism that has been named order by disorder [12]. The classical ground state has still a macroscopic manifold, which could be removed by quantum fluctuations [9]. On the other hand, there are predictions of a disordered ground state, a quantum spin liquid with singlet formation for the  $S = 1/2$  kagomé AF [13].

The topology of the classical ground state degeneracies has been analysed in more detail in Monte Carlo (MC) simulations of the 2D Heisenberg AF by Reimers and Berlinsky [11]. An intriguing result of these simulations is (an indication of) a divergence of the spin-correlation

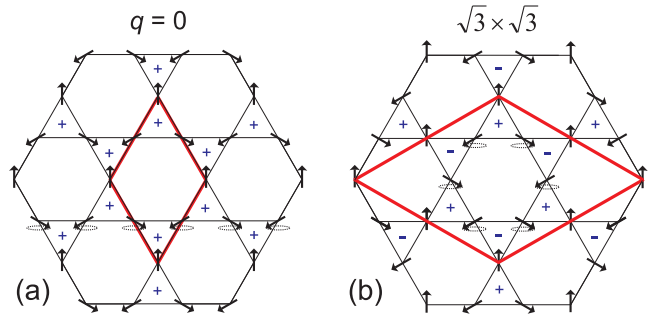


FIG. 1: (color online). In nitely degenerate AF ground states on the kagomé lattice. (a) the  $q=0$  structure with uniform chirality; (b) the staggered chiral structure, which has a larger unit cell by  $\sqrt{3} \times \sqrt{3}$ . Chirality is denoted by signs inside the triangles. The dashed ellipses represent thermal fluctuations of zero energy: (a) common spin rotations in an infinite chain; (b) the weathervane defect, a common local spin rotation on the hexagon around the axis of the spins on the edges of the unit cell.

function for  $T \rightarrow 0$  K towards an ordered ground state resembling the  $\sqrt{3} \times \sqrt{3}$  structure, whereas chiral long-range order appears to be prohibited by disorder due to the local common zero energy spin rotations as depicted in Fig. 1.

Experimental studies of the 2D kagomé AF are difficult and rare, although pyrochlores [14], magnetoplumbites [15], and jarosites [16, 17, 18] contain layers of the kagomé structure. For weak interlayer coupling, these candidates combine all the desired ingredients: low dimensionality, low coordination, and strong frustration. A neutron scattering study on magnetoplumbite  $SrCr_{8-x}Ga_{4+x}O_{19}$  [15] provided the first experimental evidence of short-range spin correlations down to 1.5 K and indicated a preference for the  $\sqrt{3} \times \sqrt{3}$  structure. The jarosite  $(D_3O)_Fe_3(SO_4)_2(OH)_6$  stays disordered even at low  $T$  according to diffuse neutron scattering data (obtained with polarization analysis), but the ordering wave vector could

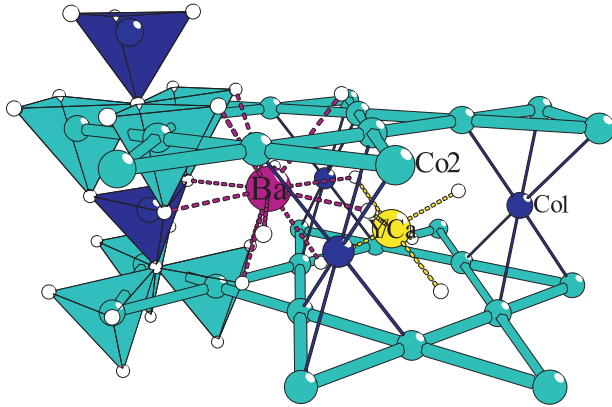


FIG. 2: (color online). The average crystal structure of  $Y_{0.5}Ca_{0.5}BaCo_4O_7$ . Thicker lines between the  $Co_2$  atoms highlight the kagomé layers. All Co atoms are tetrahedrally coordinated by oxygen, as shown in the polyhedral representation (left), emphasizing the three-fold symmetry axes, going through  $Co_1$  (blue), which allow trimization of  $Co_2$  in the kagomé substructure.

not be clearly identified. Another close realization of the kagomé AF is the jarosite  $KFe_3(SO_4)_2(OH)_6$ , although the interference of 3D Néel order below 65 K complicates comparisons to the ground state properties of the kagomé AF. Recent single crystal studies show spin correlations towards the  $q_0$ -structure [17], contrary to theoretical expectations for the kagomé AF with only nearest neighbor interactions. Indeed, small AF interactions to next nearest neighbors, which have been deduced from the low energy spin wave excitations [18], stabilize the  $q_0$ -structure instead of an order by disorder mechanism. More interestingly, the low energy spin wave excitations could be related to the "zero energy modes" as shown in Fig. 1 (a) [18].

Here, we present results of diffuse neutron scattering with polarization analysis on a new compound  $Y_{0.5}Ca_{0.5}BaCo_4O_7$ , a realization of the kagomé AF with only nearest neighbor interactions, which allows an unprecedented approach to its ground state properties.

The average crystal structure of  $Y_{0.5}Ca_{0.5}BaCo_4O_7$  is known [19, 20] (Fig. 2) and a mixed valence of  $Co^{2+}$  and  $Co^{3+}$  is a consequence of stoichiometry. Co occupies two different tetrahedral sites in the structure: 75% of all Co ( $Co_2$ ) constitute the kagomé layers and the remaining 25% fill the  $Co_1$  sites, which are on threefold axes between the kagomé layers. Within this symmetry, a trimization in the kagomé layers is possible and different  $Co_2$ - $Co_2$  bond lengths are in fact observed at 300 K [20]. Because of shorter Co-O distances, the valence of  $Co_1$  must be higher than that of  $Co_2$ , indicating a preference for  $Co^{3+}$  ( $3d^6$  configuration). The bonding situation and spin state of  $Co^{3+}$  seem to be responsible for two dimensional magnetic behavior: (i) geometrically, the tetrahedral coordination causes a high frustration for

any possible AF exchange between the kagomé layers; (ii) the possibility of a low spin state of  $Co^{3+}$  at the interlayer sites, as  $Co^{3+}$  is situated closer to a trigonal plane changing the point-group symmetry from  $T_d$  to  $C_{3v}$ . According to Hund's rules, an ideal tetrahedral coordination with weak crystal field splitting (oxygen ligands) results in high spin states, on the other hand low spin states have been observed for  $C_{3v}$  symmetry [21, 22].

Polycrystalline  $Y_{0.5}Ca_{0.5}BaCo_4O_7$  samples for the diffuse neutron scattering experiments have been synthesized by a solid-state reaction in air [20]. Under the applied synthesis conditions, the oxygen stoichiometry should be ideal as verified by iodometric titration on the parent compound  $YBaCo_4O_7$  [23]. The scattering experiments were performed on the DNS instrument in Jülich. In contrast to most previous investigations [14, 15, 17], the magnetic scattering was separated from nuclear scattering by polarization analysis [16, 25]. A fortiori, the separated high background due to nuclear spin-incoherent scattering from Co serves as an intrinsic calibration of the paramagnetic cross-section; a procedure that avoids usual systematic errors and corrections. A strong diffuse peak evolves upon cooling and its asym-

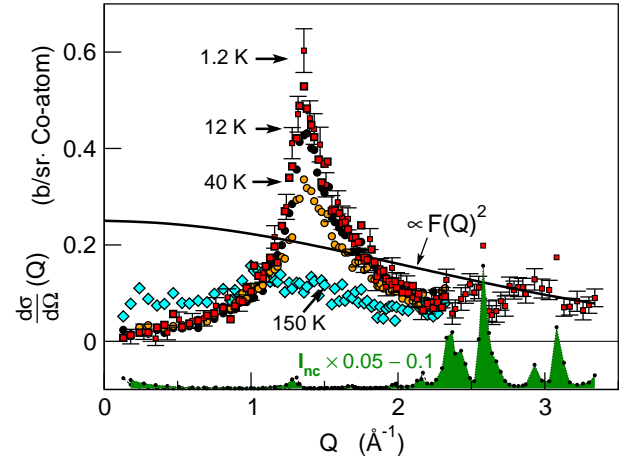


FIG. 3: (color online). Separation of scattering contributions and temperature dependence of the separated diffuse magnetic scattering; data are calibrated by the separated spin-incoherent scattering of Co (0.382 b/sr); the separated nuclear coherent scattering,  $I_{nc}$  has been rescaled and shifted (bottom part).

metric shape indicates low dimensional spin correlations (Fig. 3). Remarkably, no long-range magnetic order appears even at very low T. The magnetic scattering can be described in terms of the Fourier transform of the spin pair-correlations, applying orientational averaging for the polycrystalline sample [24]. For a direct comparison with the MC results, we use a simplified scattering expression [11], which neglects a possible interrelationship between

spin correlation and spin direction:

$$\frac{d}{d_{\text{mag}}} = \frac{2}{3} \frac{e^2}{m_e c^2} F_Q^2 \frac{X}{r} hS_0 S_r i \frac{\sin Q r}{Q r}; \quad (2)$$

Here, the product of the classical electron radius ( $e^2/m_e c^2 = 0.282 \times 10^{-12} \text{ cm}$ ) and the neutron gyromagnetic ratio = -1.91 defines the magnetic scattering length  $r_0 = 0.54 \times 10^{-12} \text{ cm}$ ;  $m_e$  is the electron mass,  $e$  is its charge, and  $c$  is the velocity of light.  $S$  represents the spin quantum number of the scattering ion,  $F_Q$  denotes the magnetic scattering form-factor of the single ion  $\text{Co}^{2+}$ . For the ideal paramagnet,  $T = J$ , the scattering is purely elastic and proportional to the self-correlation  $S(S+1)$ . In general, one has to consider the expectation value of the time-dependent self-correlation function of a spin precessing in the strong local field of its neighbors. For  $T = J$  and integrating over only small energy transfers in direction, the expectation value reduces effectively to that of the scalar product of the ordered moments  $hS_z^2 i$ .

The magnetic scattering intensity allows us to estimate the average Co spin moment. A fit to the 12 K data yields a forward scattering of 0.25(2) b/sr Co for the self-correlation term. The best quantitative agreement is found if we assume that  $\text{Co}^{2+}$  ions (5/8 of all Co) are in high spin state  $S = 3/2$  and that  $\text{Co}^{3+}$  ions (3/8 of all Co) are in low spin state  $S = 0$  yielding 0.273 b/sr Co-ion. It is clear that  $S = 0$  at the Co1 sites rationalizes the absence of any significant interlayer coupling and, hence, the ultimate suppression of 3D long-range order.

The dielectric scattering probes the wave-vector dependent susceptibility  $\chi(Q) = \frac{1}{r} hS_0 S_r i \frac{\sin Q r}{Q r}$ , where  $\hat{S}$  are spins of unit length. Within the approximation made for Eq. (2), the 12 K data are compared with the MC results in Fig. 4. Correlations between the directions of the spins and their distance vector would require higher order corrections neglected in Eq. (2). In case of the  $\text{P}\bar{3}\text{P}\bar{3}$  structure, as shown in Fig. 1(b), we analyzed that this would result in significant intensities for  $0 < Q r < 1$ , for nearest neighbor distances  $j_1 j = a/2$  and a unit cell parameter  $a = 6.30 \text{ \AA}$ , which is in contradiction to our observations. According to Eq. (1), the Hamiltonian is degenerate with respect to a common spin rotation in the kagomé plane, and we conclude that this degeneracy is essentially preserved.

Furthermore, we can rule out spin correlations towards the  $q_0$ -structure, whose ordering wave vectors are  $a(h,k)$ ; the strongest peak would be at  $Q = \frac{p}{a} j = \frac{p}{a} (1,0) j = 1.152 \text{ \AA}^{-1}$ , where  $a = (2\sqrt{3})/3$ . Instead of this, the observed peak coincides with  $Q = \frac{p}{a} q \frac{p}{a} j = \frac{p}{a} (1=3;1=3) j = 1.330 \text{ \AA}^{-1}$ , the ordering wave vector of the  $\text{P}\bar{3}\text{P}\bar{3}$  structure.

The data has been analyzed in terms of spin correlations by a Fourier analysis using a linear least squares

fit. The results are shown in the inset of Fig. 4, where the spin correlations have been normalized to the correlation function of the ideal  $\text{P}\bar{3}\text{P}\bar{3}$  structure:

$$G^{\text{P}\bar{3}}(r) = h\hat{S}_0 S_r i \cos q^{\text{P}\bar{3}} r; \quad (3)$$

which equals to unity when the spins are in the  $\text{P}\bar{3}\text{P}\bar{3}$  conformation. A limited number of parameters could be determined, which clearly show the preference for building up the  $\text{P}\bar{3}\text{P}\bar{3}$  structure.

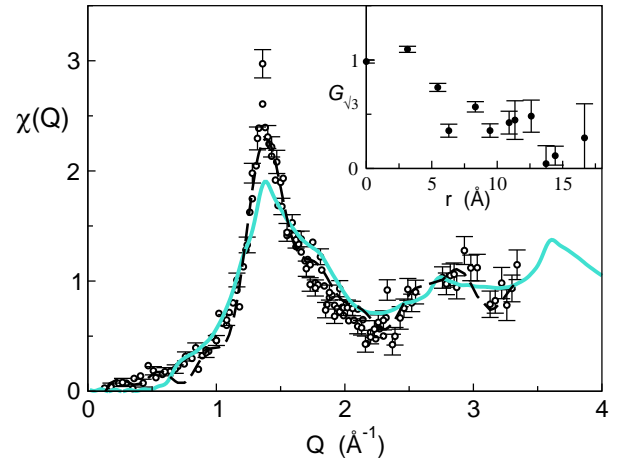


FIG. 4: (color online). Susceptibility  $\chi(Q)$  from 12 K data versus modulus of wave vector  $Q$ ; the thick (cyan) line represents MC data from Ref. [11], for a classical Heisenberg AF at  $T/J = 0.002$ ; dashed line represents a fit of the spin correlation by Fourier analysis, whose results, as normalized to correlations in the ideal structure,  $G^{\text{P}\bar{3}}$ , are shown in the inset.

An interesting question is whether our data can provide any indication for the proposed weathervane defects (cf. Fig. 1(b)) that seem to disturb the chiral long range order of the ground state in the previous MC simulations. Therefore, one may compare a model of the ideal  $\text{P}\bar{3}\text{P}\bar{3}$  structure to a defect model, and convolute the correlations with an adjustable asymptotic decay function. A simple defect model is to place the weathervane defects on two of the three sublattices. Note that the configurational average of this model is equivalent to a collinear structure model, and that the correlations are reduced by a factor 2 with respect to the ideal structure ( $h\hat{S}_0 S_r i = 1$  or  $= 1/2$ ) for distances exceeding the spacings that occur within the unit cell. An algebraic decay of the correlations has been found in MC simulations [11], which relates the spin correlations to a percolation phenomenon. However, the present data are affected by instrumental resolution (see Fig. 3 separated nuclear scattering) such that we cannot reliably distinguish between an exponential and algebraic decay. Models based either on the ideal structure or on the weathervane defect are in close agreement with the data. The exception is that

both models produce a small additional peak at  $q = \frac{\pi}{3}$ , an integral intensity that is one order of magnitude weaker than the peak at  $2q = \frac{\pi}{3}$ . The discrepancy is less significant, approximately half the size, if the weathervane defects are included. Apparently, the spin structure is even less ordered and a more appropriate model would include that weathervane defects are distributed on all sublattices. Therefore, MC simulations are adequate to sample the conformational space. Indeed, there is a qualitatively astonishing agreement between our data and the MC results [11] for the classical Heisenberg AF. In particular, MC simulations reproduce the absence of the peak at  $q = \frac{\pi}{3}$ . The disorder has been related to a structure of chiral domains with anti-phase boundaries. According to the MC data, the correlation length of chiral order parameter stays short ranged for  $T = 0$  K, while the spin correlation length and the peak at  $2q = \frac{\pi}{3}$  diverge in this limit. It is noteworthy that this observed peak, as compared to the MC simulation, is significantly more pronounced. Hence, the ground state is approached much closer in our experiment, although temperature and Curie-Weiss constant of approximately 2200 K [4J 20] matches closely the conditions of the simulation,  $T=J=0.002$ . In fact, the peak is affected by the instrumental resolution and the true peak height is already substantially reduced.

The weathervane defects (see Fig. 1(b)) are local collective spin excitations of zero energy according to Eq. (1) that preserve the sum of spins and give rise to residual entropy in analogy to ice [27] and spin-ice systems [14]. Local collective spin excitations have also been observed in inelastic neutron scattering from cubic spinel  $ZnCr_2O_4$  [26]. Very recently, "chain-like" excitations (from the  $q_0$ -structure, see Fig. 1(a)) are lifted to finite energies by Dzyaloshinskii-Moriya (DM) interaction as been reported from inelastic neutron scattering [18]. We performed additional time-of-flight experiments verifying that the scattering at 1.2 K is essentially elastic, and proving that the spin correlations are frozen within the energy resolution of 0.5 meV. At higher temperatures, the inelastic scattering appears gapless, indicating the absence of anisotropies related to DM interaction, and exhibits a quasi-elastic broadening similar to the observations on  $SrCr_3-xGa_{4+x}O_{19}$  [15].

The strong AF exchange in the plane causes a dynamic response at high energies, which suggests that the low-energetic relaxations correspond to thermally spin fluctuations out of the kagomé plane. Theoretically, the complex free energy landscape of the kagomé AF will induce very slow spin dynamics similar to ordinary spin glasses [28] and may explain observed field cooling effects at 370 K [20].

To conclude, the present neutron study with polarization analysis on a new compound, realizing the  $S = 3/2$  kagomé AF, agrees in surprising detail with the complexity of the classical ground state for only nearest neighbor interactions as has been found in previous MC simulations.

The remarkable survival of only short-range 2D spin correlations at low temperatures is due to severe geometrical frustration by tetrahedral coordination combined with high/low spin states of Co ions in alternating layers. Site disorder with spin dilution, albeit beyond the site percolation threshold [29], results from assuming ionic bonding and from exchange of moments through electron hopping. Covalency effects might restore the predicted behavior in the experiment, which implies a long-range ordered ground state with only short-range chiral order.

We thank J.N. Reimers and A.J. Berlinsky for providing us with their original MC data.

- 
- [1] N.D. Mermin and H.W. Kramers, *Phys. Rev. Lett.* **17**, 1133 (1966).
  - [2] R. Moessner, A.T. Ramirez, *Physics Today* **59**, 24 (2006); J.E. Gudeman, *J. Mater. Chem.* **11**, 37-52 (2001).
  - [3] H. Kawamura, *J. Phys. Condens. Matter* **10**, 4707 (1998).
  - [4] V.P. Pankhtya et al., *Physica B, Proceedings of ICNS 2005* appearing in July (2006); V.P. Pankhtya et al., *Phys. Rev. B* **64**, 1000402 (R) (2001).
  - [5] J.M. Tranquada et al., *Nature* **429**, 534 (2004).
  - [6] P.A. Lindgard, *Phys. Rev. Lett.* **95**, 217001 (2005).
  - [7] I. Syozi, *Prog. Theor. Phys.* **6**, 306 (1951).
  - [8] Sachdev, S., *Phys. Rev. B* **45**, 12377 (1992).
  - [9] T. Yildirim, *Tr. J. of Phys.* **23**, 47 (1999).
  - [10] D.A. Huse, and A.D. Rutenberg, *Phys. Rev. B* **45**, 7536 (1992).
  - [11] J.N. Reimers and A.J. Berlinsky, *Phys. Rev. B* **48**, 9539 (1993).
  - [12] J. Villain, R. Bidaux, J.-P. Carton and R. Conte, *J. Phys. (France)* **41**, 1263 (1980).
  - [13] C. Zeng and V. Elser, *Phys. Rev. B* **51**, 8318 (1995).
  - [14] M.J. Harris et al., *Phys. Rev. Lett.* **79**, 2554 (1997).
  - [15] C. Broholm, G. Aeppli, G.P. Espinosa, and A.S. Cooper, *Phys. Rev. Lett.* **65**, 3173 (1990).
  - [16] A.S. Wills et al., *Phys. Rev. B* **64**, 094436 (2001).
  - [17] D. Roholka et al., *Nature Mater.* **4**, 323 (2005).
  - [18] K. Matan et al., *Phys. Rev. Lett.* **96**, 247201 (2006).
  - [19] M. Valldor and M. Andersson, *Solid State Sci.* **4**, 923 (2002).
  - [20] M. Valldor, accepted for publication in *Solid State Sci.* (2006); cond-mat/0605063.
  - [21] E.K. Byrne, D.S. Richeson, and K.H. Theopold, *J. Chem. Soc., Chem. Commun.* **19**, 1491 (1986).
  - [22] D.M. Jenkins et al., *J. Am. Chem. Soc.* **124**, 15336 (2002).
  - [23] M. Karppinen, et al., *Chem. Mater.* **18**, 490 (2006).
  - [24] I.A. Blech and B.L.A. Verbach, *Physics* **1**, 31 (1964).
  - [25] W. Schweika, S. Easton, and K.-U. Neumann, *Neutron News* **16**, 14 (2005).
  - [26] S.-H. Lee, *Nature* **418**, 856 (2002).
  - [27] L. Pauling, *The nature of the chemical bond*, Cornell U. Press, Ithaca, NY (1945).
  - [28] M. Ferrero, F. Becca, and F. Mila, *Phys. Rev. B* **68**, 214431 (2003).
  - [29] M.F. Sykes and J.W. Essam, *J. Math. Phys.* **5**, 1117 (1964).